

Supporting information

UV- and NIR-Protective Semi-Transparent Smart Windows Based on Metal Halide Solar Cells

Karunakara Moorthy Boopathi,[†] Chintam Hanmandlu,^{†, ‡} Anupriya Singh,^{†, §} Yang-Fang Chen,[§] Chao Sung Lai,[‡] and Chih Wei Chu^{*, †, ||, §}

[†]*Research Center for Applied Science, Academia Sinica, 128 Academia Road, Sec. 2, Nangang, Taipei 115, Taiwan (R.O.C).*

[‡]*Department of Electronic Engineering, Chang Gung University, No. 259, Wenhua 1st Road, Guishan District, Taoyuan City 33302, Taiwan (R.O.C.).*

[§]*Department of Physics, National Taiwan University, No. 1, Sec. 4, Roosevelt Road, Taipei 106, Taiwan (R.O.C.).*

^{||}*College of Engineering, Chang Gung University, No. 259, Wenhua 1st Road, Guishan District, Taoyuan City 33302, Taiwan (R.O.C.).*

[§]*Department of Materials Science and Engineering, National Tsing Hua University, Hsinchu 30013, Taiwan (R.O.C.)*

^{*}*E-mail: gchu@gate.sinica.edu.tw*

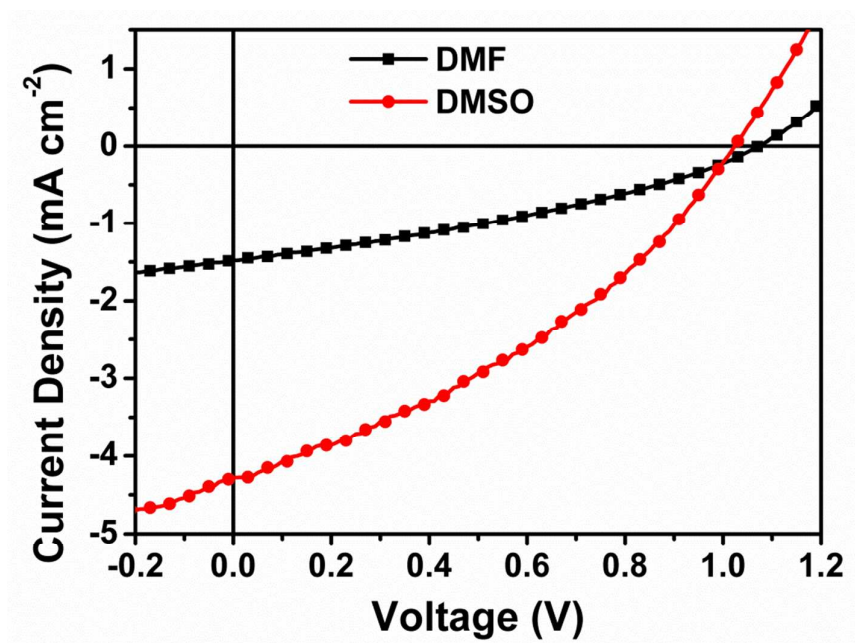


Figure S1 J - V characteristics of $\text{PbI}_2/\text{N2200}$ hybrid solar cells featuring an opaque electrode (Ca/Al), with the PbI_2 films prepared using different solvents.

Table S1 Photovoltaic performance parameters of $\text{PbI}_2/\text{N2200}$ hybrid solar cells featuring an opaque electrode (Ca/Al), with the PbI_2 films prepared using different solvents.

PbI_2 Solvent	V_{oc} (V)	J_{sc} (mA cm^{-2})	FF (%)	PCE (%)
DMF	1.07	1.48	34.2	0.54
DMSO	1.02	4.28	35.7	1.56

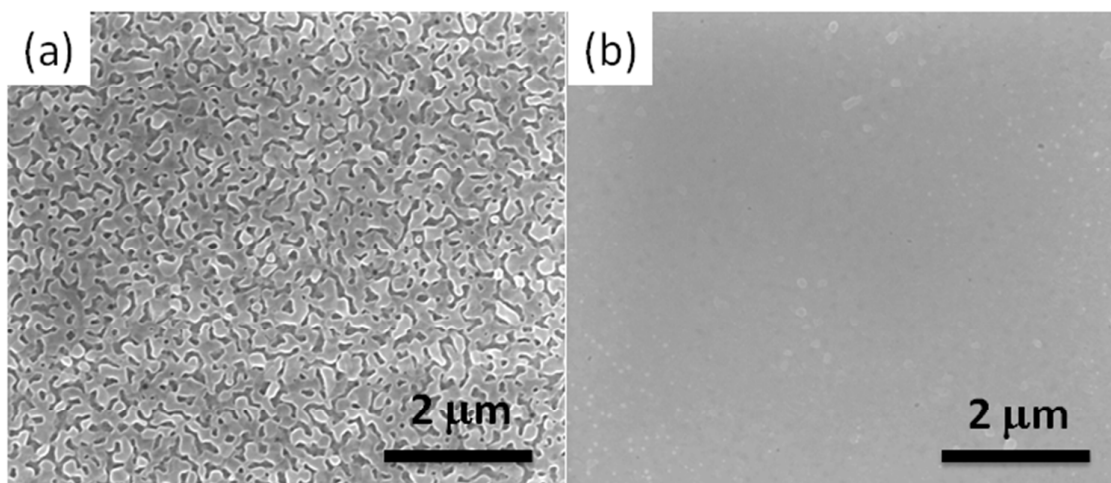


Figure S2 Top-view SEM images of annealed PbI_2 film prepared on ITO/PEDOT:PSS using (a) DMF and (b) DMSO as solvents.

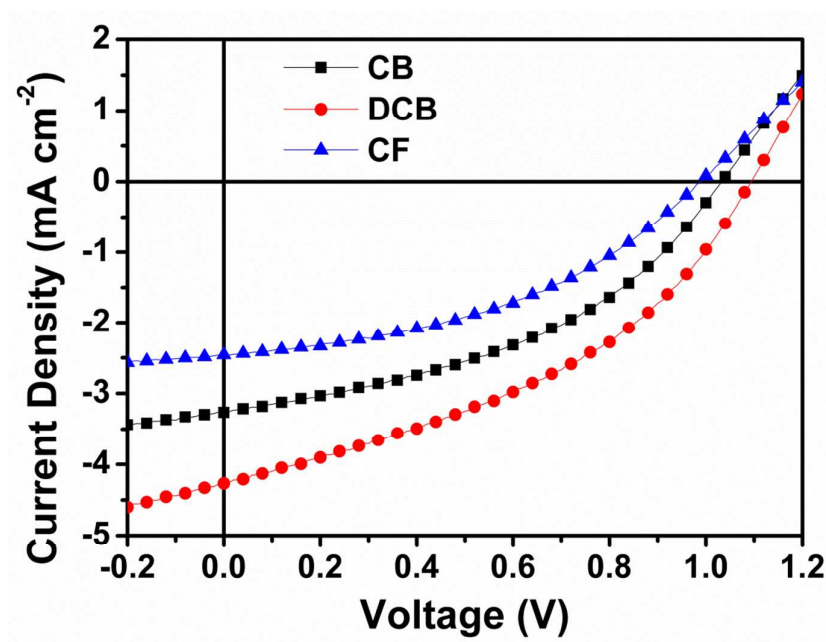


Figure S3 J - V characteristics of PbI_2 /N2200 hybrid solar cells featuring an opaque electrode (Ca/Al), with the N2200 films prepared using different solvents.

Table S2 Photovoltaic performance parameters of $\text{PbI}_2/\text{N2200}$ hybrid solar cells featuring an opaque electrode (Ca/Al), with the N2200 film prepared using different solvents.

N2200 Solvent	V_{oc} (V)	J_{sc} (mA cm^{-2})	FF (%)	PCE (%)
CB	1.03	3.27	42.5	1.43
DCB	1.09	4.27	39.8	1.85
CF	0.99	2.46	42.3	1.03

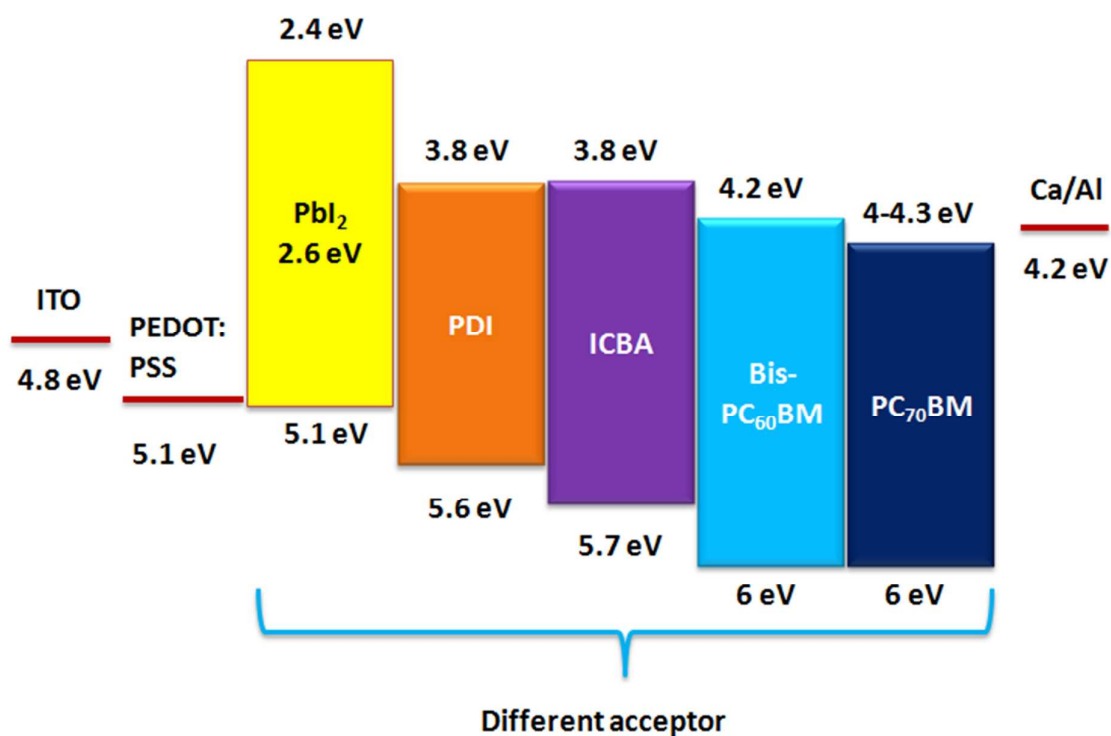


Figure S4 Energy band diagram of PbI_2 -based solar cells featuring an opaque electrode (Ca/Al) and various acceptor materials.

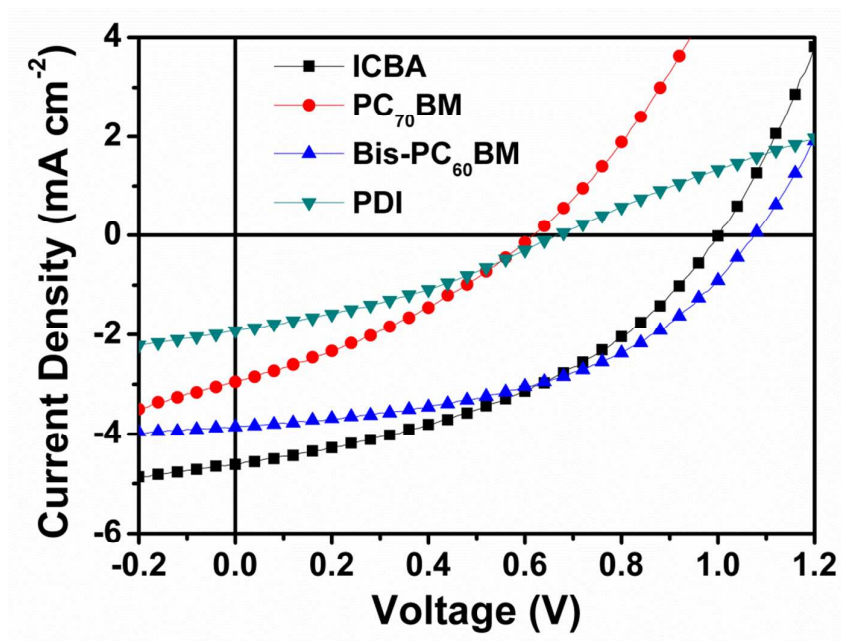


Figure S5 J - V characteristics of PbI_2 -based hybrid solar cells featuring an opaque electrode (Ca/Al) and various acceptor materials.

Table S3 Photovoltaic performance parameters of PbI_2 -based hybrid solar cells featuring an opaque electrode (Ca/Al) and various acceptor materials.

Acceptor material	V_{oc} (V)	J_{sc} (mA cm^{-2})	FF (%)	PCE (%)
ICBA	1.00	4.62	41.1	1.90
PC ₇₀ BM	0.62	2.95	32.8	0.60
Bis-PC ₆₀ BM	1.02	4.86	38.5	1.91
PDI	0.67	1.92	33.4	0.43

Table S4 Photovoltaic performance parameters of $\text{PbI}_2/\text{N2200}$ solar cells featuring an opaque electrode, measured under light intensities ranging from 100 to 10 mW cm^{-2} .

Light intensity (mW cm^{-2})	V_{oc} (V)	J_{sc} (mA cm^{-2})	FF (%)	PCE (%)
100	1.02	4.28	35.7	1.56
80	1.01	3.48	36.4	1.60
60	1.00	2.64	36.0	1.58
40	0.98	1.78	36.7	1.60
20	0.94	0.93	35.1	1.55
10	0.91	0.61	34.3	1.90

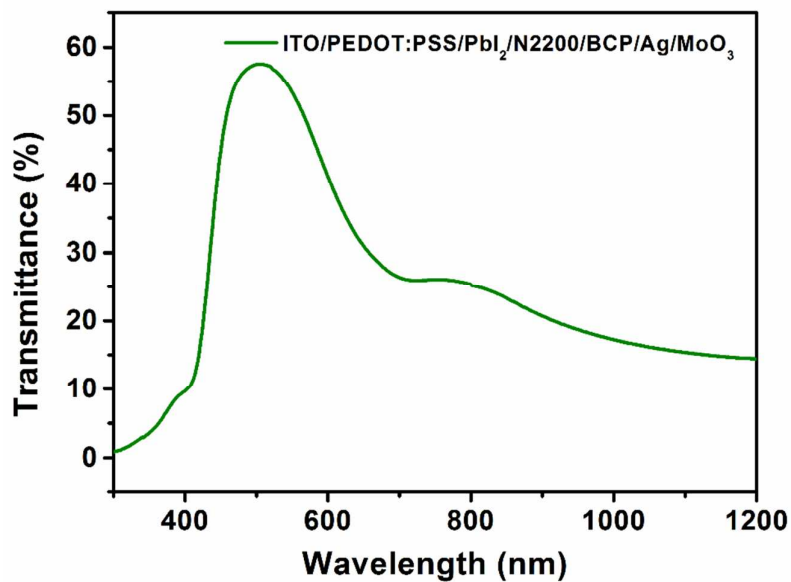


Figure S6 Transmittance of whole device featuring with transparent electrode (BCP/Ag/MoO_3) which clearly showed the Near-IR (NIR) light is absorbed effectively by BCP/Ag/MoO_3 electrodes.

Table S5 Photovoltaic performance of PbI_2 solar cell illuminated with light on two sides: front-side illumination intensity was set at 1 sun, while variable light intensity was applied for rear-side illumination.

Light intensity (sun)	V_{oc} (V)	J_{sc} (mA cm^{-2})	FF (%)	PCE (%)
1	0.62	2.97	35.8	0.66
1+0.1	0.66	3.45	36.5	0.75
1+0.2	0.67	3.63	37.0	0.76
1+0.4	0.69	4.20	37.6	0.78
1+0.6	0.71	4.65	38.2	0.79
1+0.8	0.72	5.17	39.0	0.81
1+1	0.74	5.60	39.1	0.81

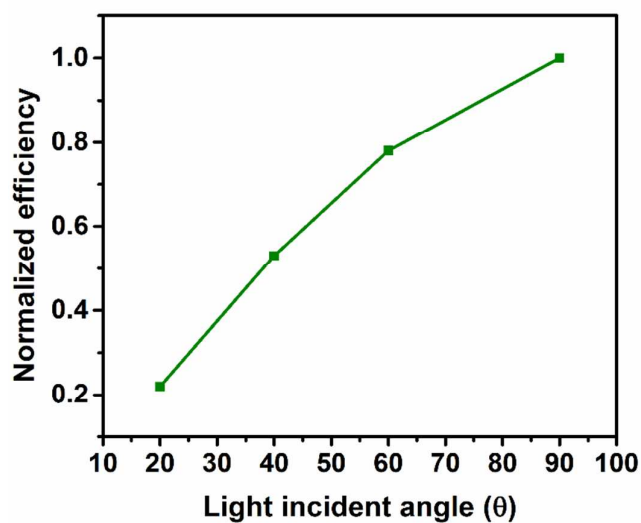


Figure S7 Normalized device performance of PbI_2 -based hybrid solar cells featuring a transparent electrode at different light incident angle from 20 to 90°.

We studied the influence of the incident angle of light on the device performance because of the alteration of the incident angle of sunlight during a day. Figure S7 showed that normalized efficiency of PbI_2 based hybrid solar cell with respect to incident angle. We achieved the maximum performance when device is normal (90°) to the incident light angle. The device performance was reduced while changing the angle.

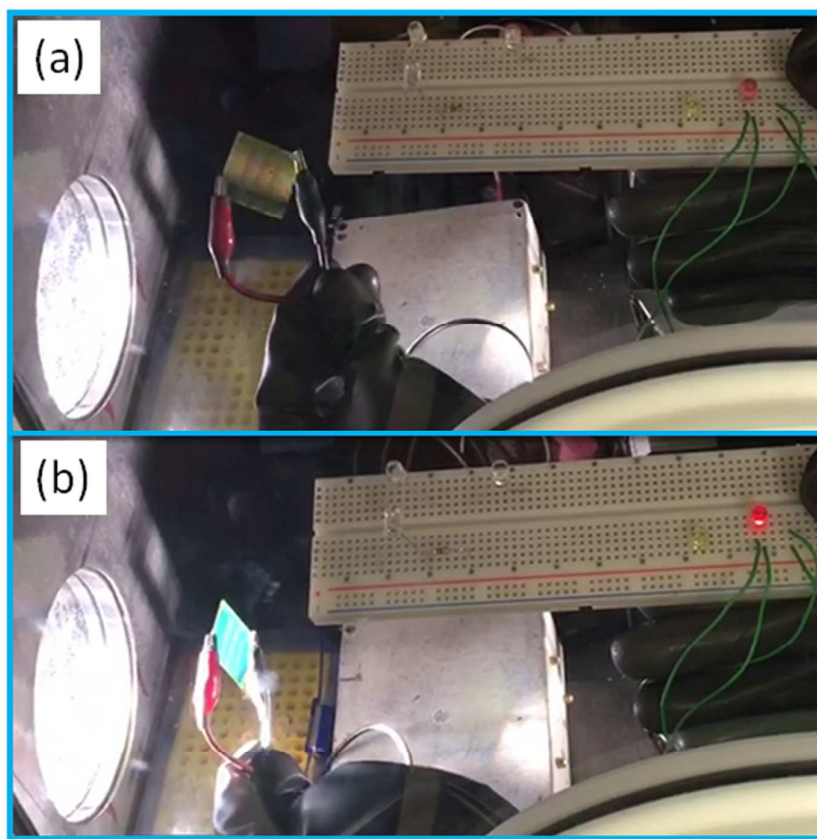


Figure S8 LED lit up by a large-area semitransparent PbI_2 solar cell fabricated with a transparent top electrode ($\text{BCP}/\text{Ag}/\text{MoO}_3$); (a) without and (b) with sun illumination.